ELSEVIER

International Journal of Fatigue 23 (2001) 207–214

International Journal of Fatigue

www.elsevier.com/locate/ijfatigue

Static strengthening and fatigue blunt-notch sensitivity in low-carbon steels

M.D. Chapetti [a,*], N. Katsura [b], T. Tagawa [b], T. Miyata [b]

[a] *INTEMA, University of Mar del Plata, J.B. Justo 4302 (7600) Mar del Plata, Argentina*
[b] *Material Science and Engineering, Nagoya University, Nagoya, 464-01, Japan*

Received 17 September 1999; received in revised form 28 August 2000; accepted 26 September 2000

Abstract

The influence of four different static strengthenings on the fatigue blunt-notch sensitivity of a low-carbon steel with a ferrite–pearlite microstructure was analyzed and modeled. The analysis was made using a model previously derived which estimates the fatigue limit of blunt notched components by means of the parameter k_{td} defined as the stress concentration introduced by the notch at a distance d from the notch root surface equal to the distance between microstructural barriers. While the distance d between microstructural barriers is kept constant by keeping constant the grain size, the effective resistance of the microstructural barriers to crack propagation is increased by static strengthening. The analyses have shown the influence of the distribution and effective resistance of the first two or three microstructural barriers on fatigue blunt-notch sensitivity. © 2001 Elsevier Science Ltd. All rights reserved.

Keywords: Fatigue limit; Blunt notches; Fatigue notch sensitivity; Microstructural barriers

1. Introduction

Engineering structures invariably contain stress concentrations which are the principal sites for the inception of fatigue flaws. The stress fields in the immediate vicinity of the stress concentration have a strong bearing on how the fatigue cracks nucleate and propagate. There exists now sufficient experimental evidence showing that the fatigue limit of polycrystalline metals represents the critical conditions for the propagation of nucleated cracks, and this holds both for smooth and notched specimens [1–13]. Thus, whichever is the mechanism of microcrack nucleation, the minimum stress level leading to failure (i.e. the fatigue limit) is given by the stress requirements for the propagation of the most critical microcrack.

The depth of cracks present after exposure to stress levels just below the fatigue limit was found to depend on the stress concentration factor (k_t) [3,5,6,8,12]. In "sharp" notches (high k_t), physically-small non-propagating cracks exist at the fatigue limit of the notched component (PSC, crack length less than that at which crack closure is fully developed [10]), whereas "blunt" notches (small k_t), exhibit microstructurally-short non-propagating cracks (MSC, crack length of the order of the microstructural dimensions). In both cases the length of the non-propagating cracks increases as k_t increases.

In the case of blunt notches the stress that is sufficient to initiate a crack at the notch root and overcome the strongest microstructural barrier is also sufficient to cause continuous propagation of the crack to failure, and the fatigue strength is given by a microstructural threshold determined by a $\Delta\sigma$ criterion [1,10,12,13]. On the other hand, in the case of sharp notches the fatigue strength is given by a mechanical threshold defined by a ΔK criterion, and the development of mechanical non-propagating cracks is allowed by the existence of a stress gradient high-enough and the development of the crack closure effect. In this case the fatigue strength becomes independent of the stress concentration factor k_t and is governed mainly by the notch depth D and the fatigue threshold $\Delta\sigma_{th}$ for physically small or long cracks [3,4,7].

* Corresponding author. Tel.: +00-54-23-81-6600; fax: +00-54-23-81-0046.
E-mail address: mircod@fi.mdp.edu.ar (M.D. Chapetti).

PII: S0142-1123(00)00093-1

In a previous work [12], a model for the blunt-notch size effect was derived on the basis of the experimental evidence that both the plain- and the blunt-notched fatigue limit represents the threshold stress for the propagation of the nucleated microstructurally short cracks. The derived relationship characterizes the fatigue notch sensitivity by means of the parameter k_{td} defined as the stress concentration introduced by the notch at a distance d from the notch root surface equal to the distance between microstructural barriers, as follows:

$$k_{td}=\frac{k_t}{\sqrt{1+\frac{4.5d}{\rho}}} \tag{1}$$

where ρ is the notch radius.

Defining d_i as the mean distance between microstructural barriers i, and $\Delta\sigma_{ed_i}$ as the fatigue limit associated to the same barrier i, the fatigue limit $\Delta\sigma_e$ of the notched component at a given k_t would be given by the greatest $\Delta\sigma_{ed_i}$ at that k_t, as follows:

$$\Delta\sigma_e|_{k_t}=\max\Delta\sigma_{ed_i}|_{k_t}=\max\left[\frac{\Delta\sigma_{e0d_i}\sqrt{1+4.5\frac{d_i}{\rho}}}{k_t}\right]_{k_t} \tag{2}$$

and

$$\Delta\sigma_{ed_i}=\frac{\Delta\sigma_{e0d_i}}{k_{td_i}} \tag{3}$$

with

$$k_{td_i}=\frac{k_t}{\sqrt{1+4.5\frac{d_i}{\rho}}} \tag{4}$$

where $\Delta\sigma_{e0d_i}$ is the effective resistance of the barrier i and k_{td_i} is the stress concentration introduced by the notch at a depth $x=d_i$. The concept is shown schematically in Fig. 1 by considering three consecutive microstructural barriers spaced at a distance d_1, d_2 and d_3 from the surface ($d_1<d_2<d_3$), with their effective resistance $\Delta\sigma_{e0d_1}$, $\Delta\sigma_{e0d_2}$ and $\Delta\sigma_{e0d_3}$, respectively. From $k_t=1$ to k_{t1} the fatigue limit of the notch component is given by $\Delta\sigma_e=\Delta\sigma_{e0d_1}/k_{td_1}$, from k_{t1} to k_{t2} by $\Delta\sigma_e=\Delta\sigma_{e0d_2}/k_{td_2}$, and so on.

In this work this concept was used to analyze the influence of four different static strengthening on the blunt-notch sensitivity of a low-carbon steel with a ferrite–pearlite microstructure. While the distance d between microstructural barriers is kept constant by keeping constant the grain size, the effective resistance of the microstructural barriers to microstructurally short crack propagation is increased by static strengthening.

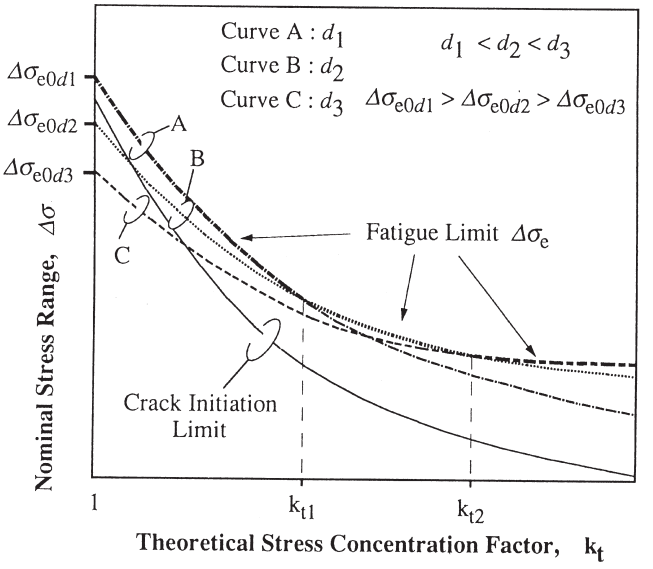

Fig. 1. The fatigue limit $\Delta\sigma_e$ of blunt notches defined as the greatest fatigue limit associated with the effective resistance $\Delta\sigma_{e0d_i}$ and the position from the notch-root surface d_i of the microstructural barriers i — see Eq. (2).

2. Materials, specimens and testing conditions

Five different steel compositions were analyzed: NUBase; NUNi; NUSi; NuCu; and NUCoP. Their compositions and mechanical properties are shown in Tables 1 and 2, respectively. All the microstructures are ferrite–pearlite with the same grain size (55 μm). They were obtained by laboratory remelting up to 1200°C and then hot rolled. Steel NUBase had the base composition. Steels NUNi and NUSi were solution hardened with 2.23% nickel and 1.96% Si, respectively. Steels NUCu and NUCuP were solution hardened with 1.52 and 1.56% of Cu, respectively. Steel NUCuP was then subjected to ageing treatment of 500°C for 2 h. An additional increase in tensile strength of 30% was observed by this treatment (precipitation hardening), compared with steel NUCu.

Three different bar tensile specimens were tested (see Fig. 2). One of them with plain surface while the other two with blunt notches. According to the results from finite element methods the values of the theoretical concentration factor k_t in notched specimens were 1.94 and 2.51. After machining, the notches were mechanically polished with a series of grits down to 1 μm diamond paste. All fatigue test specimens were chemically etched in 3% Nital before being tested. The specimens were analyzed after testing with a SEM.

Constant stress amplitude tests under axial loading with zero mean stress and 30 Hz frequency were carried out in an Instron fatigue test machine. All tests were performed at room temperature in laboratory air. The fatigue limit $\Delta\sigma_e$ was defined as the maximum nominal stress under which a specimen endured $>10^7$ cycles. The

Table 1
Chemical compositions of steels tested (wt%)

Steel	C	Si	Mn	P	S	Cu	Ni	Al	N
NUBase	0.12	0.04	0.80	0.003	0.001	0.00	0.01	0.025	0.003
NUNi	0.10	0.04	0.79	0.003	0.001	0.00	**2.23**	0.029	0.003
NUSi	0.10	**1.96**	0.79	0.003	0.002	0.00	0.01	0.024	0.003
NUCu	0.10	0.04	0.81	0.003	0.002	**1.52**	0.01	0.029	0.003
NUCuP	0.10	0.04	0.82	0.003	0.002	**1.56**	0.01	0.028	0.003

Table 2
Mechanical properties of steels tested

Steel	σ_{uts} (MPa)	σ_Y (MPa)	E.L. (%)	*Hv*	$\Delta\sigma_{e0}$ (MPa)	$\Delta\sigma_e$ (MPa) k_t=2.51
NUBase	374	225	39.6	103	300	190
NUNi	438	284	16.1	140	430	240
NUSi	563	423	13.9	162	590	270
NUCu	518	387	29.2	164	500	280
NUCuP	646	512	25.6	214	600	290

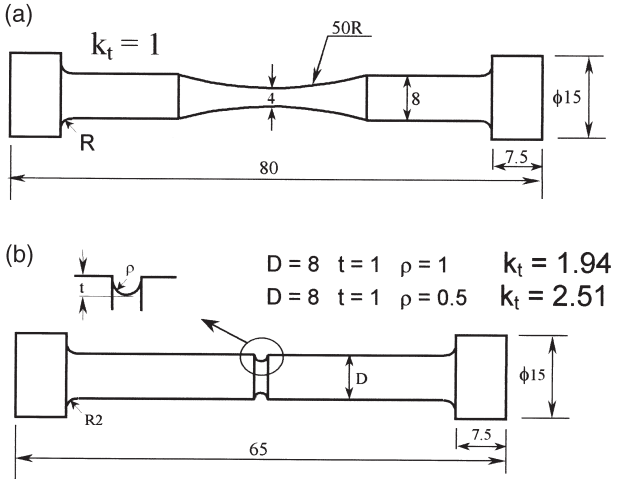

Fig. 2. Specimens, dimensions are in mm. (a) Smooth round bar specimen (k_t=1). (b) Notched round bar specimen: k_t=1.94 and k_t=2.51.

crack initiation limit $\Delta\sigma_i$ was defined as the limiting nominal stress required to develop a microstructurally-short crack. Stress level was kept constant for each tested specimen. The fatigue limit $\Delta\sigma_e$ was then analyzed by testing different specimens at different stress levels. Stress increment between two consecutive stress levels was chosen equal to 10 MPa.

3. Resistance and position of the microstructural barriers

Fig. 3(a–e) show the stress distributions ahead of the notch root corresponding to the notches analyzed, for nominal stress ranges at and below the fatigue limit and above the initiation limit of the microstructures corresponding to the steels NUBase, NUNi, NUSi, NUCu and NUCuP, respectively. Stress distributions were obtained by using finite element models of the specimens [12]. The dark oval drawings represents the microstructural barriers, and their positions in depth is defined by the average grain size of the material. The upper point of the oval drawing gives the effective resistance of the barrier for crack propagation, and was estimated as follows: the elastic stress distributions were drawn only to the depth given by the length of the longest arrested crack obtained at a given nominal stress level, and then the barriers were placed by moving it vertically and taking in main that it cannot be crossed by the stress distribution. It is worth noting that for the seek of clarity only a few stress distributions were drawn, but two consecutive stress distributions were separated by a stress level given by a nominal stress range of 10 MPa and the corresponding k_t.

In most of the cases (mainly for microstructurally short cracks) the depth *a* of the non-propagating cracks (a_{np}), was defined using the total surface length 2*c* and considering that the aspect radio *a*/*c* was about 1 (semicircular cracks), which was observed experimentally. When physically small non-propagating cracks were obtained, the specimens were fractured and the crack analyzed and measured using SEM. Fig. 4(a–e) show examples of the microstructurally-short non-propagating cracks obtained for all steels. Fig. 5 shows additional photos of non-propagating cracks obtained by fractographic and metallographic analyses. Specimens were fatigued [Fig. 5(a)] or fractured [Fig. 5(b and c)] to obtain photographs. Photo (d) shows a cross-section of a crack arrested in the first grain boundary.

Cracks usually initiate along persistent slip bands

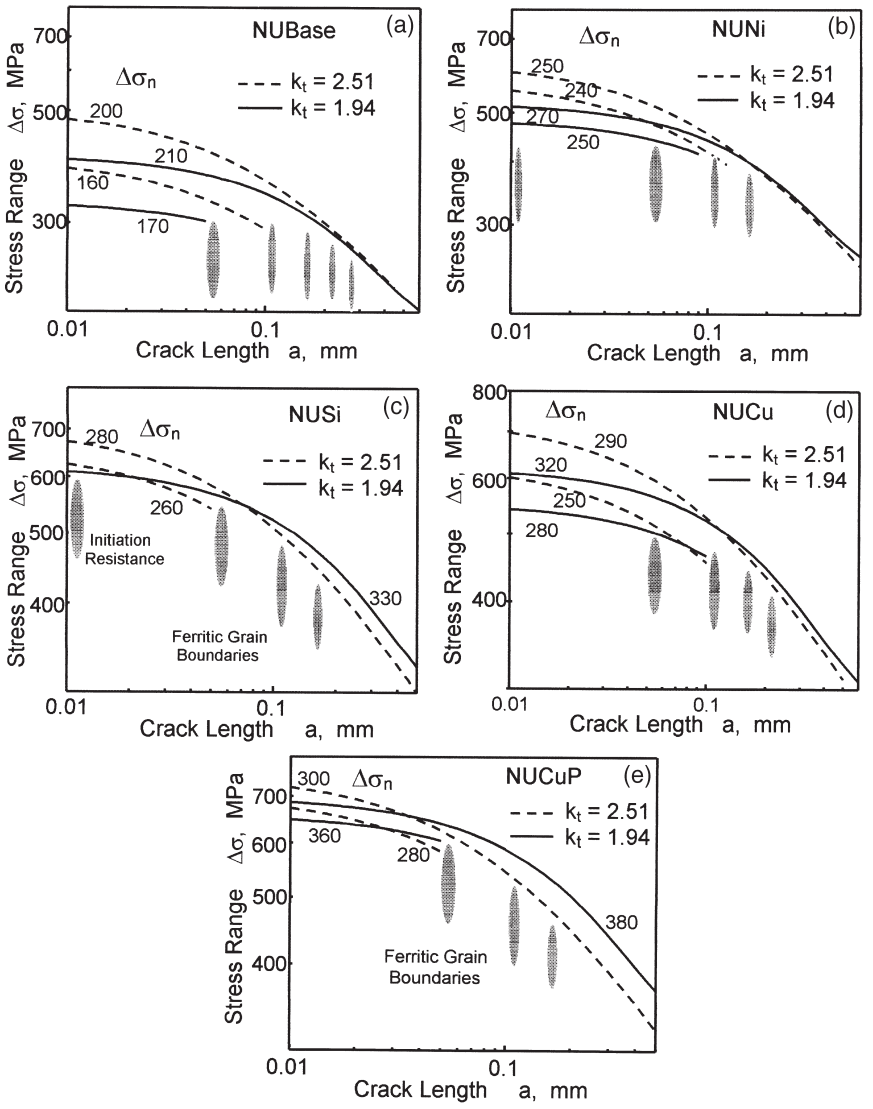

Fig. 3. Stress distributions ahead of the notch root for different nominal applied stress ranges and two stress concentration factors. (a) NUBase, (b) NUNi, (c) NUSi, (d) NUCu and (e) NUCuP. Dark oval symbols represents the position and the effective resistance of the microstructural barriers (grain boundaries).

(PSBs) proceeding in ferrite grains or along grain boundaries. In any case the grain boundaries are considered as microstructural barriers and the position given by the average size of the ferritic grains (about 55 μm), is considered as the distance between two consecutive barriers. Pearlite is also barrier to crack propagation, but the amount is small and it is usually placed in grain boundaries, as it can be seen in Fig. 5(d). In this way we obtain d_1=0.055 mm, d_2=0.11 mm, d_3=0.165 mm, and so on. The estimated effective resistance of the barriers are shown in Table 3.

4. Results and discussion

Fig. 6(a–e) show plots of the fatigue limit versus the stress concentration factor k_t, obtained experimentally for all steels. The type and nature of the non-propagating cracks obtained at several stress levels below the fatigue limit is specified. The bold line corresponds to crack initiation (k_{td}=k_t), and the dotted lines correspond to Eq. (3) for the first two or three important microstructural barriers. Experimental results are also shown. It can be seen that Eq. (3) fits the experimental data reasonably well.

In Fig. 7 all the fatigue limits $\Delta\sigma_e$ were normalized by the limits for respective unnotched specimens, $\Delta\sigma_{e0}$. The bold line means that the notch has its full theoretical effect (k_{td}=k_t). It can be seen that the notch sensitivity is clearly different for all the five steels analyzed. The highest notch sensitivity was found in NUSi, where the fatigue limit is given by the initiation of a micro-crack (k_{td}=k_t, d=0). In this microstructure the solution hardening obtained with Si increases the crack initiation resist-

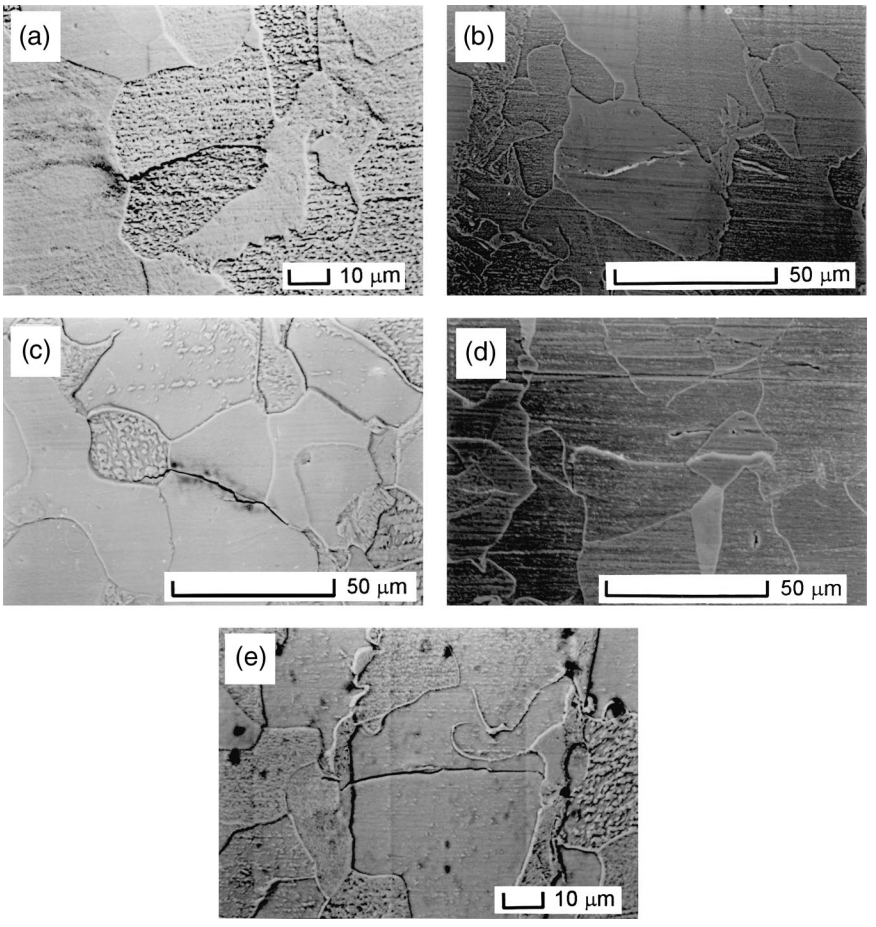

Fig. 4. Examples of surface views of microstructurally-short non-propagating cracks obtained in NUBase (a), NUNi (b), NUSi (c), NUCu (d) and NUCuP (e).

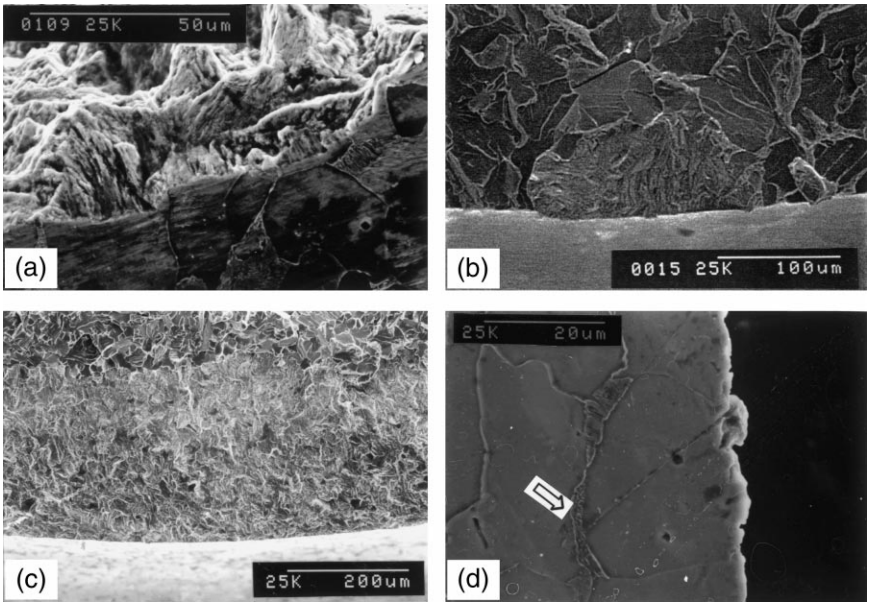

Fig. 5. Examples of non-propagating cracks. Specimens were fatigued (a) or fractured (b and c) to obtain photographs. Photograph (d) shows a cross-section of a crack arrested in the first grain boundary.

Table 3
Estimated effective resistance of the microstructural barriers

Microstructural barrier	Effective resistance (MPa)				
	NUBase	NUNi	NUSi	NUCu	NUCuP
First (d_1=55 μm)	300	425	540	500	600
Second (d_2=110 μm)	295	410	480	480	510
Third (d_3=165 μm)	285	375	425	455	450

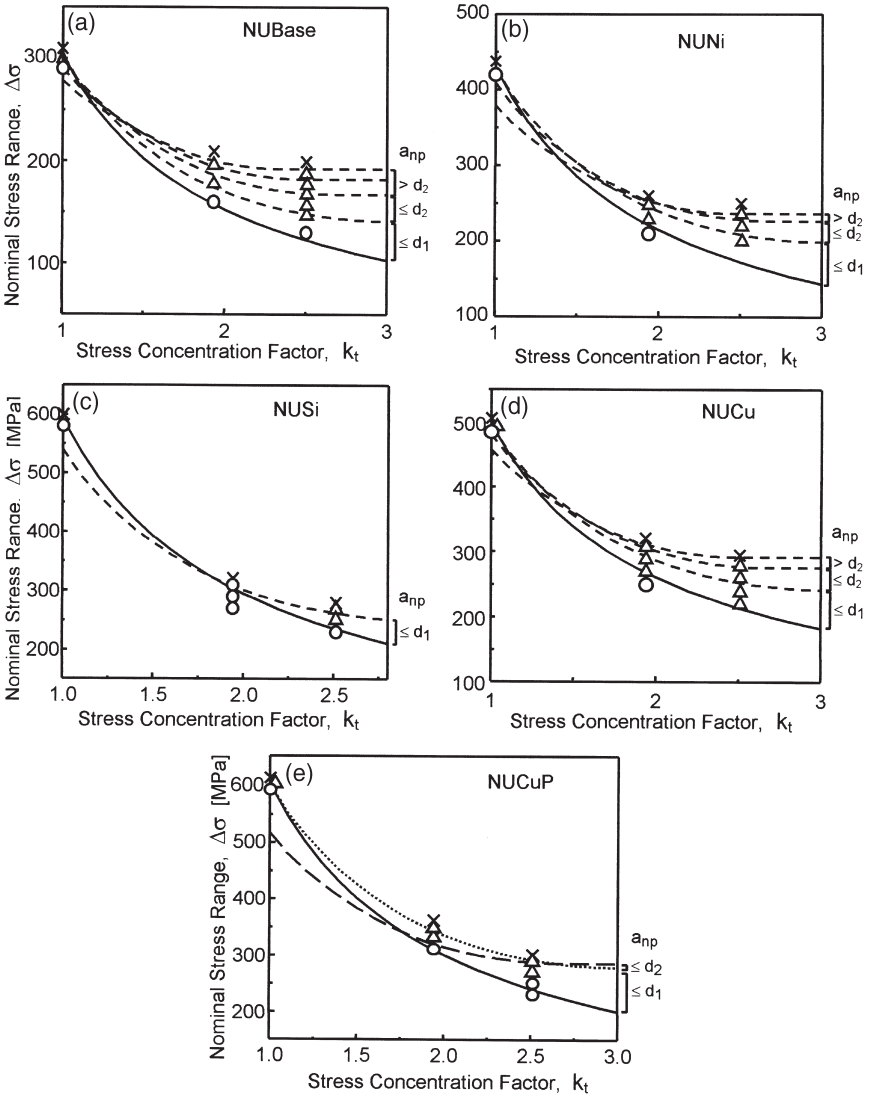

Fig. 6. Fatigue strength against theoretical stress concentration factor. ○, No cracks; △, non-propagating cracks; ×, fracture. NUBase (a), NUNi (b), NUSi (c), NUCu (d) and NUCuP (e).

ance beyond the effective resistance of the strongest microstructural barrier. The first microstructural barrier (defined as the ferritic grain boundary), starts to define the fatigue limit at k_t equal to about 1.7. Its relatively low effective resistance does not decrease significantly the notch sensitivity for higher k_t.

In NUCuP the plain fatigue limit $\Delta\sigma_{e0}$ is given by the first microstructural barrier in almost the whole k_t range

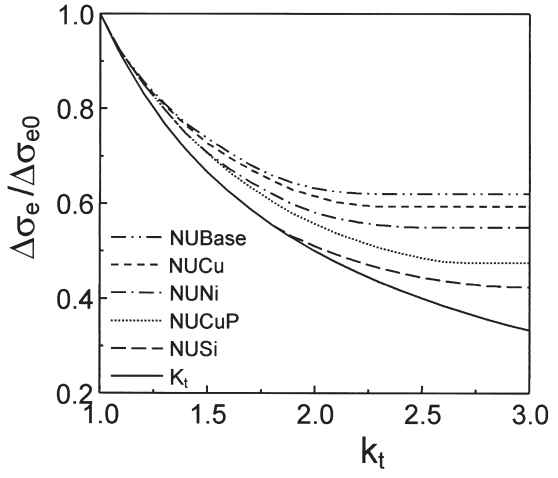

Fig. 7. Stress concentration factor against normalized fatigue limits.

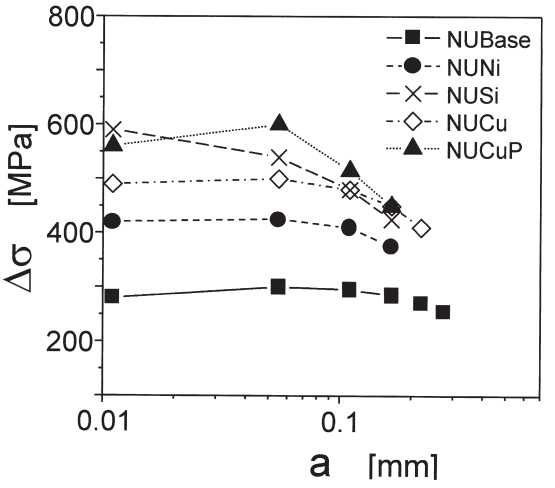

Fig. 8. Estimated distributions of the microstructural barriers for all steels analyzed. The position and the effective resistance of each barrier is characterized by a symbol.

analyzed, and the notch sensitivity is then given by k_{td_1} with d_1=55 μm.

The lowest fatigue notch sensitivity is obviously obtained for NUBase due to its quite low static and plain fatigue resistances. Following is NUCu, for which the fatigue limit is given by the first, second or the third microstructural barrier, as k_t increases.

From Figs. 3 and 6 it seems that for k_t=2 the fatigue limit is given by the first microstructural barrier in NUSi ($\Delta\sigma_e$=320 MPa), and NUCuP ($\Delta\sigma_e$=370 MPa). These two materials have similar plain fatigue limits, which are given by the crack initiation resistance in NUSi and the resistance of the first microstructural barrier in NUCuP. For k_t=1.94 the fatigue limit is given by the first barrier in both steels. The position of the first barrier (d_1) is the same in both of them, and so, the fatigue limit is given by the effective resistance of the barrier $\Delta\sigma_{e01}$, according to Eq. (3) for i=1. This effective resistance is about 60 MPa higher in NUCuP than in NUSi (see Table 3), explaining the difference observed in fatigue limit at k_t=1.94, that is, 370 and 320 MPa, respectively (see Table 3).

For k_t=2.51 the fatigue limit was given by the second or the third barrier for all steels analyzed, except for NUBase, for which the fatigue limit is given by deeper ones. Fig. 8 shows the estimated distributions of the first three or four microstructural barriers for all steels analyzed. It can be seen that the effective resistances of the second and third barriers are similar in NUSi, NUCu and NUCuP, explaining why similar fatigue limits are obtained for these steels at k_t=2.51: 270, 280 and 290 MPa, respectively (see Table 3).

In a previous paper [13], the fatigue limit of a blunt notched component was analyzed from an energetic point of view. A total crack extension force was estimated using both the local extension force, related to the surface strain concentration phenomena, and the external extension force given by the applied stress intensity factor. It was shown that the effectiveness of the first microstructural barrier is mainly related to the local crack extension force. For the second barrier both the local and the external extension forces have similar value, and for the third or deeper barriers, the external crack extension force predominates. In this case the non-propagating cracks are mainly given by a mechanical threshold defined by a ΔK criterion, and allowed by the existence of a stress gradient high-enough and the development of the crack closure effect. According to the last concept, if the fatigue limit is associated with the third or forth microstructural barriers, the amount of crack closure play an important role and can explain the differences observed at relatively high k_t (2.51).

To model the fatigue limit of notched components it is necessary to join both the microstructural and mechanical parameters. For a blunt notch, Eq. (2), together with $\Delta\sigma_{e0}$ and the position d of the first predominant microstructural barrier seems to conservatively estimate the fatigue limit. It is possible to get a fatigue resistance of the material as a function of the crack length a, starting from this point (d, $\Delta\sigma_{e0}$), following the effective resistance of the first three or four microstructural barriers and joining the mechanical threshold for long cracks given by Δk_{th}. Further work will be done in this way.

5. Conclusions

The influence of four different static strengthenings on the fatigue blunt-notch sensitivity of a low-carbon steel with a ferrite–pearlite microstructure was analyzed and modeled. While the distance d between microstructural barriers was kept constant by keeping constant the grain size, the effective resistance of the microstructural

barriers to microstructurally-short crack propagation was increased by static strengthening.

It was observed that there is an apparent limit in increasing the grain resistance to crack initiation. Above this limit the fatigue limit is defined by the crack initiation at grain boundaries and the fatigue notch sensitivity is increased.

From the analyses it can be concluded that not only the first and strongest barrier but also the distribution or the relative resistance of the first three or four ones are important parameters defining the fatigue blunt-notch sensitivity. As k_t increases, deeper microstructural barriers seem to define the fatigue limit and the non-propagating crack length.

References

[1] Smith RA, Miller KJ. Prediction of fatigue regimes in notched components. Int J Mech Sci 1978;20:201–6.
[2] Lukas P, Klesnil M. Fatigue limit of notched bodies. Mater Sci Engng 1978;34:61–6.
[3] El Haddad MH, Topper TH, Smith KN. Prediction of non propagating cracks. Engng Fract Mech 1979;11:573–84.
[4] Dowling NE. Notched member fatigue life predictions combining crack initiation and propagation. Fat Engng Mater Struct 1979;2:129–38.
[5] Tanaka K, Nakai Y, Yamashita M. Fatigue growth threshold of small cracks. Int J Fract 1981;17(5):519–32.
[6] Tanaka K, Nakai Y. Prediction of fatigue threshold of notched components. Transact ASME 1984;106:192–9.
[7] McEvily AJ, Minakawa K. On crack closure and the notch size effect in fatigue. Engng Fract Mech 1987;28(5/6):519–27.
[8] Tanaka K, Akiniwa Y. Resistance-curve method for predicting propagation threshold of short fatigue cracks at notches. Engng Fract Mech 1988;30(6):863–76.
[9] Lukás P, Kunz L, Weiss B, Stickler R. Notch size effect in fatigue. Fat Fract Engng Mater Struct 1989;12(3):175–86.
[10] Miller KJ. The two thresholds of fatigue behaviour. Fat Fract Engng Mater Struct 1993;16(9):931–9.
[11] Ting JC, Lawrence FV. A crack closure model for predicting the threshold stresses of notches. Fat Fract Engng Mater Struct 1993;16(1):93–114.
[12] Chapetti MD, Kitano T, Tagawa T, Miyata T. Fatigue limit of blunt-notched components. Fat Fract Engng Mater Struct 1998;21:1525–36.
[13] Chapetti MD, Kitano T, Tagawa T, Miyata T. Two small-crack extension force concept applied to fatigue limit of blunt notched components. Int J Fatigue 1999;21(1):77–82.